

ORIGINAL ARTICLE

Open Access



Numerical Quantification Model and Experiment of External Force on Roller Hemming of Curved Edge Aluminium Alloy with Adhesive

Jianjun Li, Wenfeng Zhu and Shunchao Wang

Abstract

Accurate quantification of external force is the key to improve the high-precision hemming of autobody closure panels. However, the mechanism of external force on forming quality of complex contour sheet metal with adhesive is not clear subjected to geometric curvature and materials. In the present study, taking the curved edge aluminum sheet as the research object, SPH (smooth particle hydrodynamics) is introduced to simulate the viscous adhesive, and the SPH-FEM (Finite element method) coupling model of adhesive and panels considering the viscosity-pressure effect is established. The numerical simulation of the roller hemming process is carried out, then the validity and reliability of the proposed method are verified by measuring the external force in real time using triaxial force sensor. The multi-step forming process and the effect of external force on the roll in/out, surface wave and plastic strain of aluminum alloy sheet under the viscosity-pressure effect are studied, and the relationship between process parameters and external force is discussed. Results show that the coupling SPH-FEM model can well reflect the hemming process of curved edge structure. The normal force is about 2–3 times of the tangential force in the pre and final hemming process. Compared with the case without adhesive, the surface wave of flange part of the hemming with adhesive is slightly larger. The normal force and the tangential force increase about 90 N and 30 N respectively, when the height increases by 1 mm. It provides an important basis for the accurate control of hemming trajectory and the improvement of manufacturing quality of autobody closure panels.

Keywords: External force, Forming, Adhesive, Simulation, Aluminum alloy sheet, Manufacturing quality

1 Introduction

Autobody closure panels, such as doors, hoods and deck-lids, have high requirements on the appearance accuracy of A-class surfaces, smooth contour and uniform clearance, which determines the static perception of the vehicle and affects the dynamic performance, reflecting the advanced level of manufacturing technology [1, 2]. The assemblies are mainly composed of inner and outer panels, which are connected by hemming process [3, 4]. Due

to the complex mechanical interaction between work-piece and tool, high forming quality is related to many process parameters, among which the external force is the most important factor. The external force can not only reflect the forming quality on-line, but also provide the basis for the feedback and compensation of the monitoring system. Therefore, it is of great significance to accurately quantify the external force for the complex contour panels with low density materials. With the acceleration of new model updating and shortening of trial-produce cycle, the relationship between external force and hemming quality has gradually become the focus of attention.

*Correspondence: zhuwenfeng@tongji.edu.cn
School of Mechanical Engineering, Tongji University, Shanghai 201804, China

During the hemming process, the outer panel is subject to complex external load, which is prone to quality defects, such as roll in/out, wrinkles and cracks [5–7]. The early research mainly focused on traditional hemming, such as die or tabletop hemming. Muderrisoglu et al. [8] studied the relationship between external load and punch stroke in different stages of flanging, pre hemming and final hemming. Le Maoût et al. [9] investigated effect of pre-strain on load under horizontal and vertical displacement of the blade by finite element method. With the advantages of automation and flexibility, roller hemming gradually replaced the former, which uses an roller moving along contour path driven by an industrial robot [10, 11]. Li et al. [12] predicted the change of external load with roller hemming time under cyclic stress. Thuillier et al. [13] studied the variation of external load based on different constitutive models, and indicated that the irregular variation and vibration were related to element and friction. Eduardo et al. [14] proposed an off-line compensation method of external force to reduce the influence of dimension on forming quality. Drossel et al. [15] indicated the contact form between the roller and the workpiece was constantly changing, which finally affected the force and torque of robot. It can be seen that the geometric contour is an important factor affecting the external force and forming quality.

Due to its corrosion resistance and sealing function, the adhesive is sandwiched between the inner and outer panels during the hemming process. After the subsequent baking process, the adhesive is cured and tightly attached to the panels. Thus, it has replaced the traditional spot welding to avoid the dent of the outer panel, and become an important auxiliary connection means [16, 17]. However, as a high viscosity fluid, the physical properties of adhesives are different from those of traditional metal materials, which makes numerical simulation and experimental quantification difficult. Svensson et al. [18] studied the hemming process with the adhesive for engine hood, and found that the results of simulation and experiment were quite different when simplified it. Li et al. [19] showed that the adhesive with a certain thickness had an effect on the roll in/out value. Burka et al. [20] indicated the viscous reaction was generated on the squeezing panel and affected by its composition. On the one hand, the flow of adhesive has an effect on sheet metal forming, and its effect can not be ignored. On the other hand, the obtained uniform thickness adhesive layer is conducive to the structural accuracy control. However, defects such as adhesive shortage and overflow, have adverse effects on subsequent baking process. Therefore, accurate forming of sheet metal with adhesive is a key problem in the quality control of the hemming process.

In summary, the basic research on the mechanical relationship between roller and work piece is still lacking. Affected by the coupling effect of dissimilar materials, the quantitative analysis is difficult to achieve. Thus, it is urgent to establish a quantification model to reveal its mechanism and predict forming quality, so as to provide basis for on-line monitoring, compensation and feedback of the system.

In this paper, the influence of external force on the forming quality of curved edge aluminum alloy sheet AA6016 is studied. SPH is introduced to simulate the viscous adhesive in flow state, and FEM is used to simulate the aluminum alloy sheet. The SPH-FEM coupled numerical model is developed, then the reliability of the simulation model is verified by the real-time monitoring of external force using triaxial mechanical sensor. The changes of normal force and tangential force in different stages with adhesive and without adhesive are studied, and the effects on roll in/out and elastic-plastic strain are discussed. Finally, the relationship between process parameters and external force is studied.

2 Modeling of Hemming with Adhesive Based on SPH-FEM

2.1 SPH Model of Hemming Adhesive

After being rapidly squeezed, the adhesive flows in the gap between the inner and outer panels. There is no fixed flow field, so it is difficult to quantify accurately. The traditional fluid-solid coupled method of Euler and FEM is difficult to track the free interface of adhesive during the roller hemming. Therefore, the meshless SPH method is introduced to simulate the adhesive, which is suitable for solving large deformation and hydrodynamics problems [21]. Coupled with the FEM, it has been successfully applied in many fluid-solid coupling fields because of its high efficiency [22]. Therefore, the same method can be used to solve the problem of the roller hemming with adhesive.

SPH uses particles to represent liquids and assigns all physical and mathematical properties of fluids to SPH particles. SPH approximately calculates the field variables of any point in the support domain by point interpolation, as shown in Figure 1.

The smooth function $f(x_i)$ and its derivatives are expressed as follows [21]:

$$f(x_i) = \sum_{j=1}^N \frac{m_j}{\rho_j} f(x_j) \cdot W(|x_i - x_j|, h), \quad (1)$$

$$\nabla \cdot f(x_i) = - \sum_{j=1}^N \frac{m_j}{\rho_j} f(x_j) \cdot \nabla_i W(|x_i - x_j|, h), \quad (2)$$

where m_j and ρ_j denotes mass and density respectively; W is the smooth kernel function, and h is smooth length.

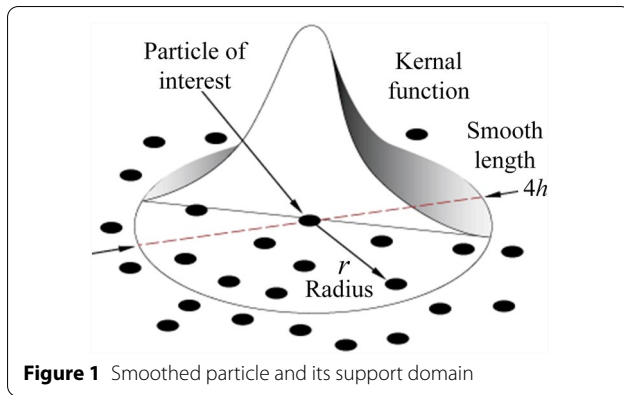


Figure 1 Smoothed particle and its support domain

The most commonly used kernel function is cubic B-spline function, defined as Eq. (3).

$$W(x - x', h) = C \begin{cases} 1 - 1.5u^2 + 0.75u^3 & 0 \leq u \leq 1, \\ 0.25(2 - u)^3 & 1 \leq u \leq 2, \\ 0 & u > 2, \end{cases} \quad (3)$$

where C is a normalization constant. For three-dimensional problems, the value of C is $1/(\pi h^3)$.

The mass conservation and momentum conservation functions in SPH form are described as follows [24]:

$$\frac{d\rho_i}{dt} = \sum_{j=1}^N m_j (v_i^\beta - v_j^\beta) \frac{\partial W_{ij}}{\partial x_i^\beta}, \quad (4)$$

$$\begin{aligned} \frac{dv_i^\alpha}{dt} = & \sum_{j=1}^N m_j \left(\frac{p_i}{\rho_i^2} + \frac{p_j}{\rho_j^2} \right) \nabla_i W_{ij} \\ & + \sum_j m_j \frac{\mu_i + \mu_j}{\rho_i \rho_j} v_{ij}^\alpha \left(\frac{1}{r_{ij}} \frac{\partial W_{ij}}{\partial r_{ij}} \right) + f_s, \end{aligned} \quad (5)$$

where N represents the overall amount of particles in the influence region of particle i , and p_i , ρ_i , μ_i , v_i^α denote the pressure, density, viscosity and speed respectively. The vector r_{ij} represents the gap, and v_{ij}^α represents the orientation. W_{ij} denotes the smooth kernel function and f_s is the interfacial tension.

The total energy of the fluid remains unchanged, so it is still necessary to introduce the equation of state to decouple the two functions. The linear U_s - U_p Hugoniot equation of state is expressed as Eq. (6) [23].

$$p = \frac{p_0 c_0^2 \eta}{(1 - s\eta)^2} \left(1 - \frac{\Gamma_0}{2} \right) + \Gamma_0 \phi \rho_0 E_m, \quad (6)$$

where η donates the nominal volume compressive strain (equal to $1 - \rho_0/\rho$), Γ_0 is the material constant, and E_m

Table 1 Main performance parameters of the hemming adhesive

Parameters	Value
Mass density (g/cm ³)	1.45
Curing conditions (min)	180°C/30
Shear strength (MPa)	≥ 30
Main components	Epoxy resin

represents the initial value of unit internal energy. ρ_0 is the density, and c_0 is the sound velocity. U_s is shock wave velocity, and U_p is particle velocity. s is the coefficient of linear relationship between U_s and U_p .

The automotive hemming adhesive studied is a one component epoxy resin type adhesive. As a polymer fluid, it mainly shows tensile flow during the squeezing process, therefore the non-Newtonian characteristics of time dependence and shear rate are ignored. At room temperature, it is simplified as high viscous Newtonian fluid. The hemming adhesive type studied is BOND-TAPE TB902, and its material parameters are provided by the manufacturer, as shown in Table 1. Before curing, the most important factor affecting the dynamic viscosity of the one-component hemming adhesive is temperature. The viscosity is obtained by the Rotational Rheometer, and its change with temperature is shown in Figure 2. The hemming time is very short, about several seconds, and the viscosity of the adhesive changes is relatively small under constant temperature. Therefore, it is assumed to be a constant value in the roller hemming process.

2.2 FEM Model of Metal Sheet

Sheet of AA6016 is selected as the research object, which is widely used in automobile outer panels due to high specific strength and formability. The mechanical

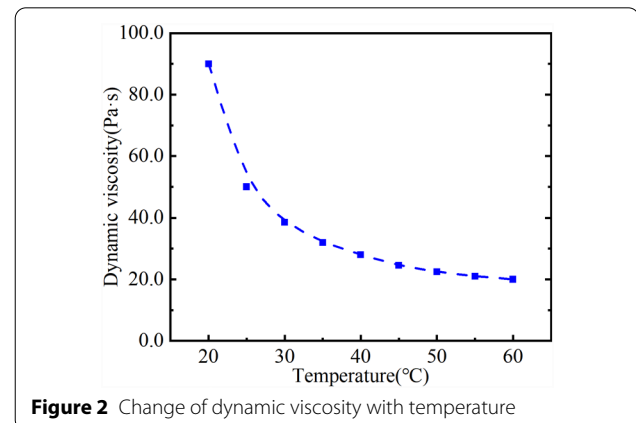


Figure 2 Change of dynamic viscosity with temperature

Table 2 Major mechanical property parameters for numerical simulation

Mechanical Property	Material AA6016
Mass density	2700
Hardening index	0.28
Possion's ratio	0.3
Yield Strength (MPa)	124
Tensile Strength (MPa)	229

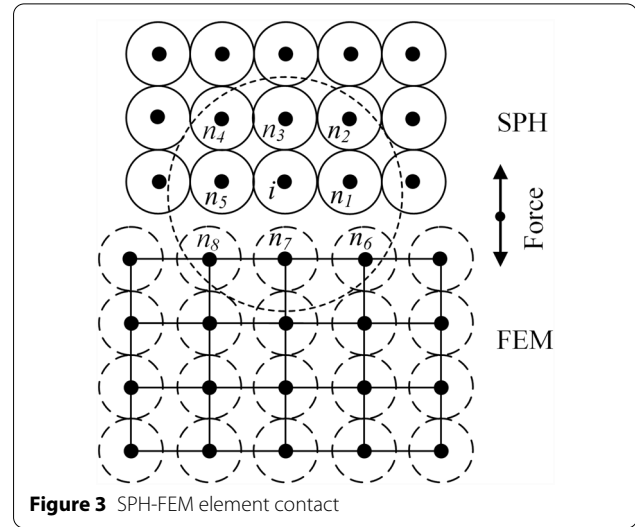
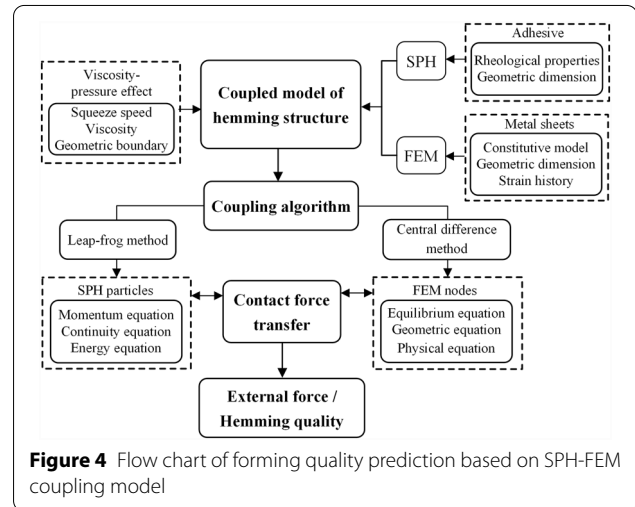
properties of the material are obtained by a conventional servo-hydraulic testing machine. Compared with the rolling direction, uniaxial tensile tests were carried out along the rolling directions of 0°, 45° and 90°. The real stress-strain curve shows that its mechanical characteristics are close to isotropy. Due to the significant fluid-solid coupling effect, the influence of the numerical model including the adhesive layer on the forming quality is much greater than that of the constitutive model of aluminum alloy. Therefore, the anisotropy of the material is not considered in the model. As the sheet metal is formed at room temperature and the hemming speed is uniform, the influence of strain rate and temperature on the material rate is ignored. Thus, an elastic-plastic power law exponential model $\sigma_p = K(\varepsilon_0 + \varepsilon_p)^n$ is considered in the numerical simulation, and the Von Mises yield criterion is adopted. The major mechanical property parameters for FEM simulation are shown in Table 2.

2.3 SPH-FEM Coupling Algorithm

FEM is a kind of Lagrangian method based on grid, which is good at calculating high-precision solid mechanics problems. SPH is a meshless Lagrangian particle method, and its accuracy is not affected by the degree of material deformation, so it is suitable for solving fluid dynamics problems. SPH and FEM have different application objects and fields, but they are complementary. The coupling of SPH and FEM can be realized by contact algorithm [21, 24], as shown in Figure 3. The contact force is added to SPH momentum equation and FEM equation in the form of external force:

$$\begin{aligned} \frac{dv^\alpha}{dt} = & \sum_{j=1}^N m_j \left(\frac{p_i}{\rho_i^2} + \frac{p_j}{\rho_j^2} \right) \nabla_i W_{ij} \\ & + \sum_j m_j \frac{\mu_i + \mu_j}{\rho_i \rho_j} v_{ij}^\alpha \left(\frac{1}{r_{ij}} \frac{\partial W_{ij}}{\partial r_{ij}} \right) \\ & + f_s + f(x_i), \end{aligned} \quad (7)$$

$$M\ddot{u} + C\dot{u} + Ku = f(x_i), \quad (8)$$

**Figure 3** SPH-FEM element contact**Figure 4** Flow chart of forming quality prediction based on SPH-FEM coupling model

where M is the structure mass matrix, C is the structural damping matrix, K is the structural stiffness matrix, and u is the displacement at a certain time.

The calculation flow of coupling algorithm is shown in Figure 4. Considering the rheological properties of adhesive and the constitutive model of sheet metal, the coupled model with different geometric contours and constraints is established. In each calculation time step, SPH particles and FEM elements transfer node information to each other through contact algorithm, including mass, position and stress. The Leap-frog algorithm is used to solve the Navier-Stokes equations of SPH particles, and the finite element difference method is used to solve the explicit dynamic equations. Finally, the deformation of metal sheet and the distribution of adhesive layer in different stages are predicted. By changing the

geometric and technological parameters, the mapping relationship between external force and forming quality is obtained.

In the numerical simulation model, the shell element is conducive to saving time and can obtain the high-precision prediction of forming quality of sheet metal [3, 25]. Compared with shell element, solid element considers the rotation and torsion of nodes, which can better reflect the interacting force. Therefore, the 8-node linear reduced integral solid element is used to simulate the outer panel. In the corner area, the mesh size is 0.3 mm. In the flanging area, the grid size is 0.5 mm, and in other areas, it is sparse. The inner panel, punch, die and roller are set as discrete rigid bodies to save calculation time. The adhesive is divided into SPH particles with the size of 0.1 mm. In the flanged stage, the distance between the punch and die is 1.3 times of the panel thickness to avoid surface indentation and large springback. Since the surface of workpiece and roller is smooth, the friction coefficient is set to 0.15 [5]. In the multi-step simulation process, the method of mass scaling is adopted, and the computer multi-core calculation is carried out based on the commercial software. Although there are many factors affecting the forming quality, such as temperature, humidity, sheet surface roughness and so on, the typical process parameters are selected, and only the action mechanism of external force under specific conditions is studied.

2.4 Experimental Conditions and Cases

The experimental equipment includes industrial robot (KUKA KR600), triaxial force sensor (omega191 f/t), roller, modular fixture and platform, etc., as shown in Figure 5. When the roller rotates, it can move along the vertical direction y and translate along the tangent direction z of the trajectory. The sensor is installed at the end of the robot arm, and the real-time data of the sensing signal is converted by the processor and transmitted to the computer. It can monitor the force in three directions at the same time.

The existence of curvature changes the forming boundary conditions, which increases the risk of defects and the difficulty of control. Therefore, a sample with typical concave edge contour is selected, as shown in Figure 6. In order to quantify the parameters conveniently, different sections are divided on the curve sample, which are evenly distributed at equal angles, S_1, S_2, \dots, S_{13} .

Different from the straight edge sample, the material of the curved edge sample is easy to stretch or compress during the multi-step process, and obvious wrinkles or fractures may appear in the final hemming. Researches showed that the defect was related to the contour radius R_C and flanged height L_F [3, 4]. Therefore, the typical

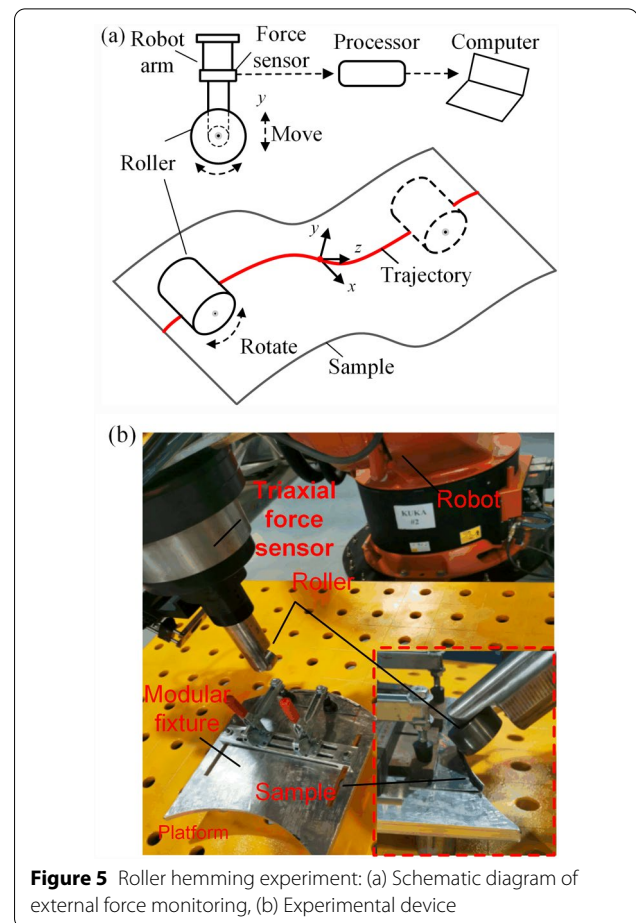


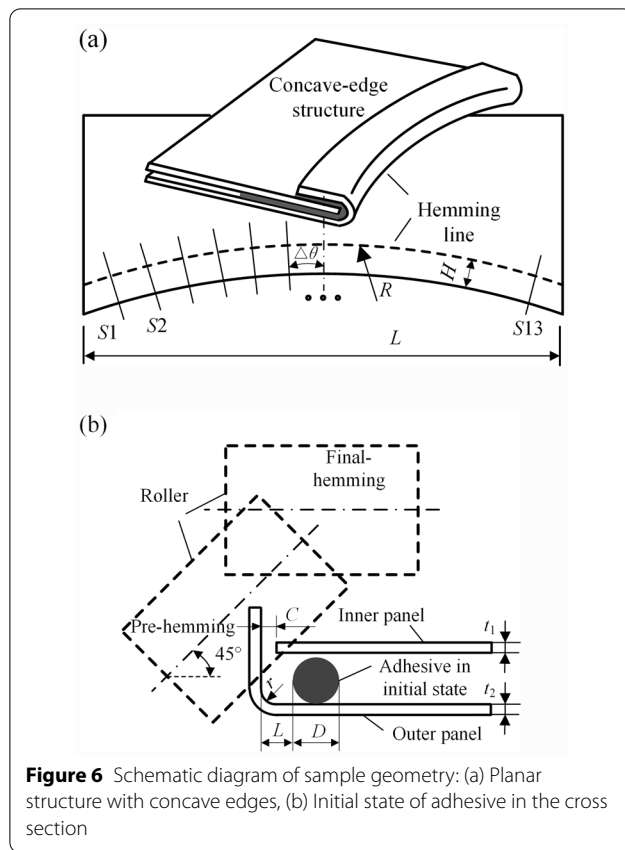
Figure 5 Roller hemming experiment: (a) Schematic diagram of external force monitoring, (b) Experimental device

structural dimensions are selected in order to ensure the final quality. The specific parameters are shown in Table 3. The roll in/out value of sample is measured by vernier caliper, three times each time, and the average value is made after experiment.

3 Results and Discussion

3.1 Comparison of Simulation and Experiment Results

As the strain history can affect the final forming quality, the flanging process is also included (Figure 7(a)). It can be seen that the outer panel has entered plastic deformation, and the strain at the corner is relatively large while the flange has been in circumferential tensile state owing to the concave edge structure (Figure 7(b)). SPH particles are used to simulate the hemming adhesive, which is cylindrical and evenly distributed along the circumferential direction (Figure 7(c)). After the inner panel is pressed vertically, the adhesive flows to the bending corner, and finally it reaches the predetermined thickness (Figure 7(d)). As the inner panel is simplified as a rigid body, there is no strain caused by the adhesive. After the pre-hemming of fluid-solid coupling interaction, there is

**Table 3** Geometric parameters of samples

Parameter names	Dimensions (mm)
Radius of edge curve R_a	240
Distance L	2.2
Distance C	1.2
Sheet thickness t_1, t_2	0.8
Flange height H	7.0
Diameter of the adhesive D	3.2
Inner flange radius r	0.8

a certain amount of adhesive accumulation at the corner (Figure 7(e)). The adhesive is extruded and flows upward, and finally it is evenly distributed in the gap between the upper and lower panels after the final hemming (Figure 7(h)). It can be seen that the coupling model can well reflect the hemming process of curved edge structure.

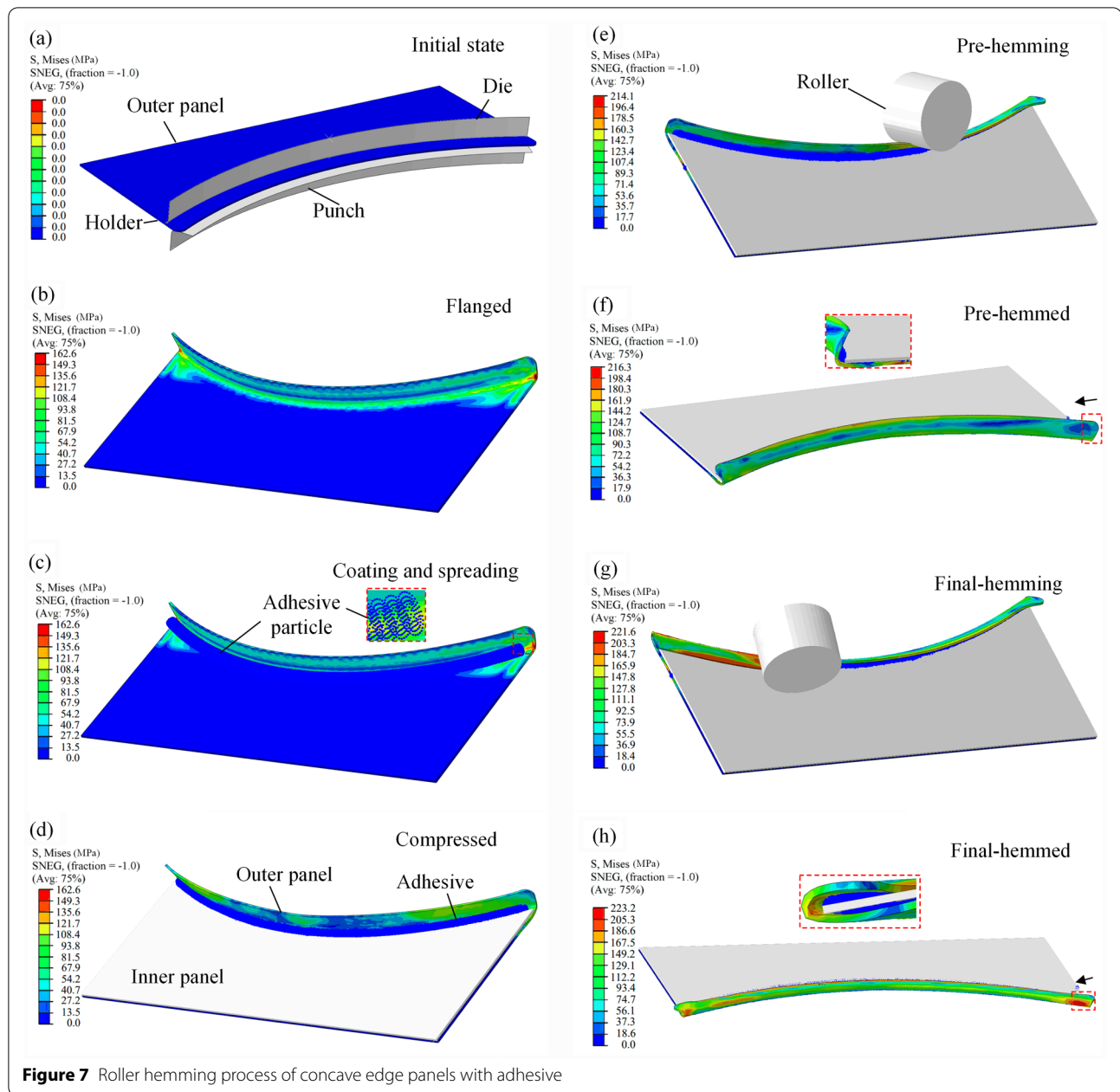
The external force is divided into the normal force perpendicular to the workpiece and the tangential force moving along the tangential trajectory. Figure 8 shows evolution of the external force in the roller hemming process by experimental and simulation methods. It can be

seen that the external force based on SPH-FEM quantification model is in good agreement with the experimental measurement results. In general, the normal force is greater than the tangential force and is the main action force. In the flanged area of sheet metal, sheet metal forming is a cycle hardening process. In the contact area with the roller, the strain of the panel is first stretched and then compressed [12]. In particular, under the viscosity-pressure effect of the adhesive, the external force obtained by simulation and experiment fluctuates in a small range. For the simulation calculation, the curve fluctuation is related to the iterative calculation under the coupling effect. According to the principle of force equilibrium, the normal force on the roller is balanced with the bending opposing force on the outer panel. It can be seen that the normal force of the sample is greater in the final hemming than that in the pre hemming. This is because the larger the bending angle and the smaller the radius of the thin panel, the greater the reverse bending moment produced. Meanwhile, with the increasing plastic deformation, material hardening occurs at the flanged part. The combined action of these factors leads to the increase of the normal force in the final hemming stage.

According to the theory of hydrodynamic lubrication [26], when the fluid is rapidly squeezed, the internal viscosity-pressure effect makes a reaction force on the solid boundaries. Therefore, compared with the sample without adhesive ($t=2.8$ mm), the outer panel of the sample with adhesive is subjected to the non-linearly transient changing viscosity-pressure at the bending corner and flanged area, resulting in a relative increase in the normal force and the tangential force. In general, the normal force is about 2–3 times of the tangential force in the two stages.

3.2 Action Mechanism of External Force

Roll in/out can affect the final assembly clearance between the panels and the autobody frame, which is an important forming quality index. Figure 9 shows the change of roll in/out in different stages. It can be seen that the roll in/out values of coupled SPH-FEM method are close to the experimental values, which can reflect the change of forming quality. In general, the outer panel retracts inward after pre hemming and then expands outward after final hemming. The reason of expand outward is mainly related to the flanged area subjected to the circumferential tensile state. The roll in values at both ends are relatively large, which is related to the free boundary conditions. Compared with the samples without adhesive ($t=2.8$ mm), the roll in values decreased, which is mainly due to the change affected by the viscosity-pressure effect. The main reason for the increase of roll in values



of samples without adhesive ($t = 2.4$ mm) is the decrease of bending radius.

Figure 10 shows the change of transient pressure and velocity of adhesive particles with time in the middle section. At room temperature, the adhesive is an incompressible fluid. After being squeezed, it flows rapidly in the narrow gap formed by the inner and outer panels, and the transient pressure appears inside. In the pre and final hemming process, there is a peak pressure, which produces a reaction force on the thin panel. The transient pressure of final hemming is different from that of pre

hemming, which is related to the gap thickness and particle velocity.

The surface flatness of the flanged part of the components not only affects the subsequent assembly quality, but also affects the distribution of the adhesive layer, which is an important forming index. Figure 11 shows the forming thickness and surface wave after the final hemming. Compared with the case without adhesive, the simulation and experimental results show that the surface wave of hemming with adhesive is slightly larger. This is related to the rapid squeeze of the adhesive layer under

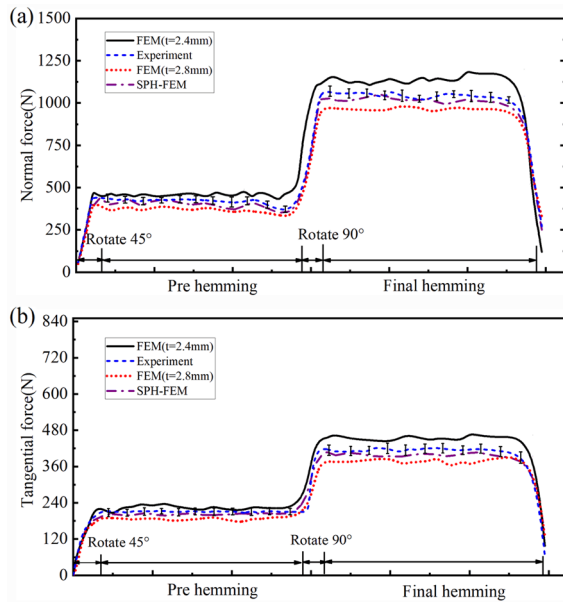


Figure 8 Evolution of external force on concave edge structure by experiment and simulation: (a) Normal force, (b) Tangential force

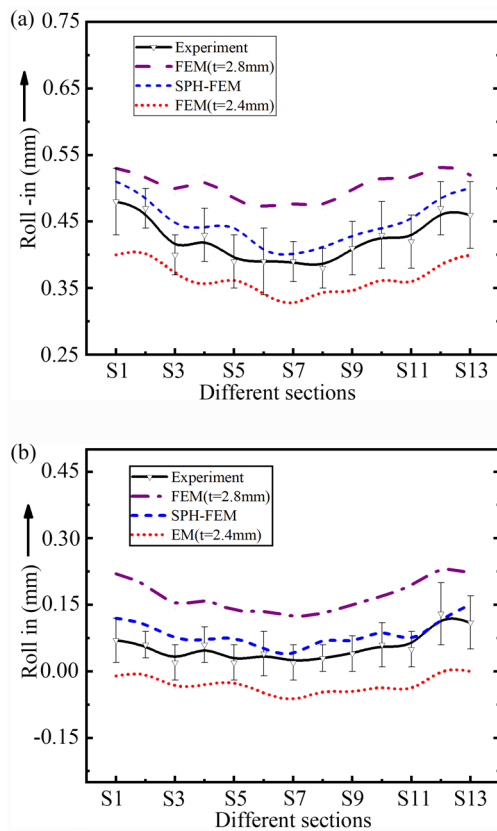


Figure 9 Changes of roll in/out at different sections: (a) Pre hemming, (b) Final hemming

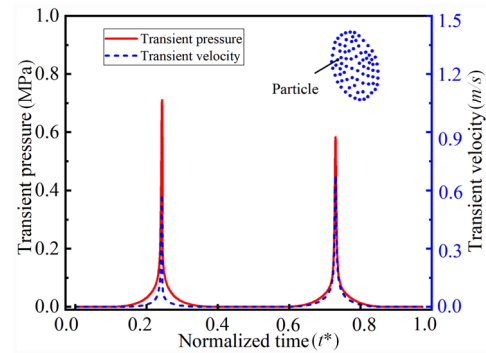


Figure 10 Transient pressure and velocity of SPH particle in the middle section

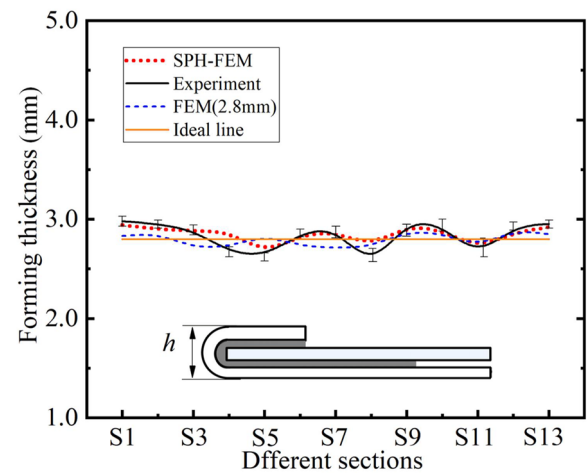
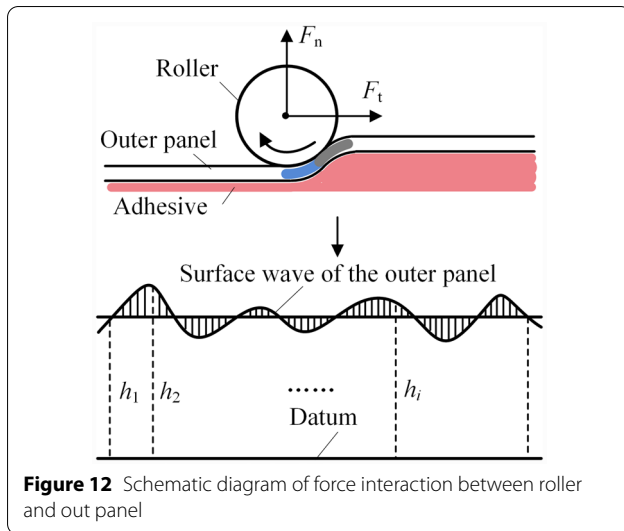


Figure 11 Forming thickness and surface wave after final hemming.

the viscosity pressure effect. The schematic diagram of force interaction between roller and out panel is shown in Figure 12. Under the action of the roller, the contact area of the sheet is first extruded and then stretched. In this extrusion region, unequal tensile stresses and strains are generated, and it eventually lead to wave wrinkling on the surface [11]. However, there is no back stress in the opposite direction, unlike the cyclic stress loading. When there is no adhesive, the outer panel is in direct contact with the inner panel with high strength, so it is easy to flatten. Influence of adhesive layer on the lower part of panel. When there is adhesive, the panel is prone to transient instability, resulting in larger wave.

Figure 13 shows the evolution of elastic-plastic behavior of samples with and without hemming adhesive. From the numerical simulation results, it can be seen that the maximum Von Mises stress of samples with adhesive is lower than that without adhesive. From the experimental results of the sample, it can be seen that the bending



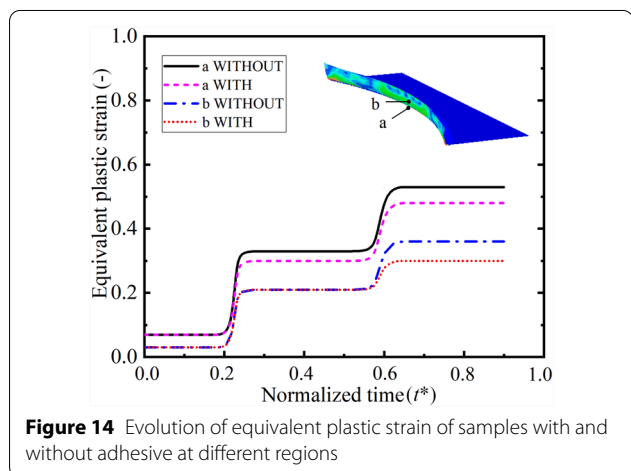
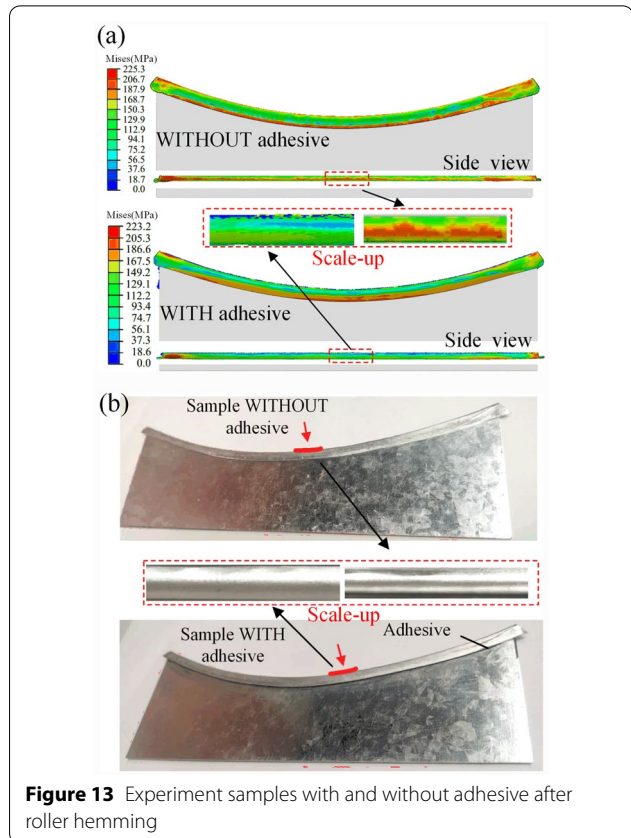
shape and surface texture in the bending area vary with the forming thickness.

From the elastic-plastic values of different points in the middle section in Figure 14, it can be seen that after flanging, the plastic strain has been produced in the thin panel, and the calculation results considering historical strain are more accurate. The equivalent plastic strain with adhesive layer is getting smaller than that without adhesive layer on the whole. This is because, on the one hand, the panel is affected by the viscosity pressure effect. On the other hand, the contact action point between the roller and the outer panel changes. The change of boundary conditions leads to the change of the normal and tangential force.

3.3 Relationship Between Process Parameters and External Force

In the roller hemming process of closure panels with complex edge contour, the pose and stiffness of the roller system change all the time. When the system is abnormal, the fluctuation of external force may increase suddenly, leading to various quality defects. In order to realize on-line monitoring, feedback and compensation, it is necessary to establish the relationship between process parameters and external force. For the convenience of comparison, the values of the external force on different sections are taken for average quantification.

The flanging height is an important forming parameter, which directly reflects the connection quality and strength. Figure 15 shows the evolution of external force with flanging height, with other parameters unchanged. It can be seen that with the increase of the height, both the normal force and tangential force increase in two



different stages. Especially in the final hemming stage, the normal force and the tangential force increase about 90 N and 30 N respectively, when the height increases by 1 mm. The main reason is that with the increase of materials in the flanging area, the reverse bending moment and tangential resistance of the outer panel increase. When the height exceeds 9 mm, the increasing rate of external

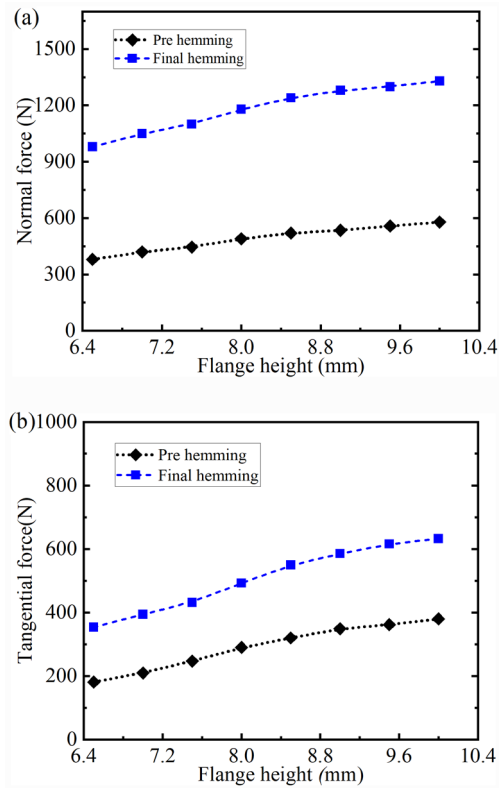


Figure 15 Evolution of external force with flanging height: (a) Normal force, (b) Tangential force

force slows down, which is related to the form of concave flanging.

The accurate control of adhesive layer thickness not only affects the flow distribution of the adhesive, but also directly affects the total forming thickness of the assembly, which is another important process parameter. Figure 16 shows the evolution of external force with the adhesive layer thickness, when other parameters remain unchanged. With the increase of thickness, the external force first increases and then decreases. When the thickness of adhesive layer is close to 0.05 mm, the external force is the largest. The smaller the extrusion thickness is, the more obvious the viscosity pressure effect is. With the increase of the thickness of the adhesive layer, the external force decreases, especially when the normal force exceeds 0.3 mm. The main reason is that with the increase of the bending radius, the bending moment of the thin panel decreases, and the influence of the adhesive decreases obviously.

The variation of the geometric contour changes the squeezing boundary conditions and also causes the change of external force. Figure 17 shows the effect of contour shape and radius on external force. In general, the external force of the curved edge sample is greater

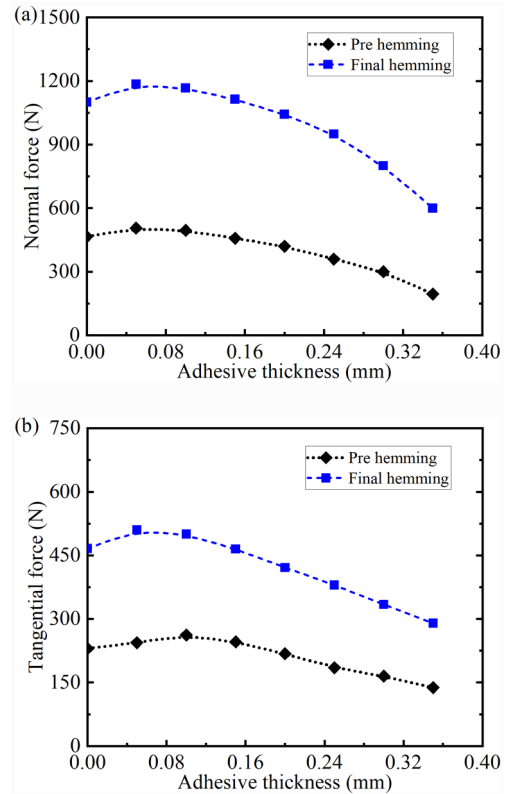


Figure 16 Evolution of external force with adhesive layer thickness

than that of the straight edge, which is related to the plastic strengthening of the flanged part with the curved edge. With the decrease of radius, the external force of the convex edge is slightly greater than that of concave edge. In the final hemming, the external force with small radius ($R=140$ mm) concave and convex edge is respectively increased by about 70 N and 100 N, compared with the straight edge. This is because materials tend to pile up on the convex edge structure when subjected to circumferential loads, requiring greater force to achieve the process thickness.

4 Conclusions

The numerical quantification model of roller hemming of curved edge AA6016 aluminum alloy with adhesive is established, and the mechanism of external force on the surface quality and gluing of adhesive is studied. Meanwhile, the relationship between process parameters and external force is studied. The main conclusions are as follows:

- (1) The coupling SPH-FEM model can well reflect the hemming process of curved edge structure. The external force based on the numerical quantifica-

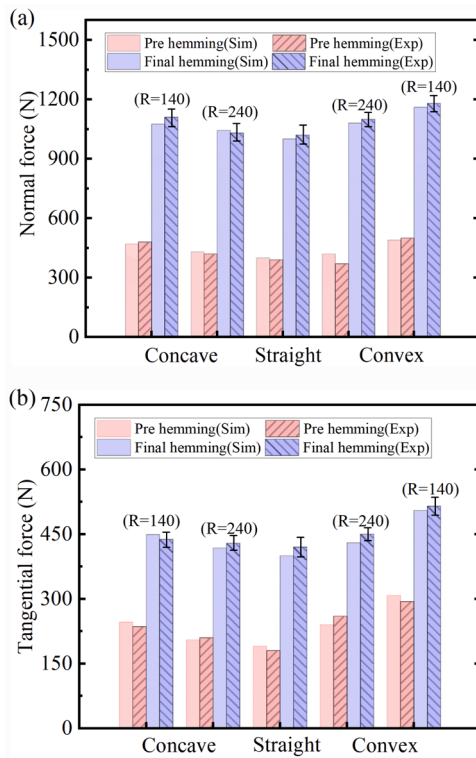


Figure 17 Influence of contour form and radius on external force

tion model is verified by experiments, which provides an effective method to obtain the external force magnitude and direction.

- (2) In general, the normal force is about 2–3 times of the tangential force in the pre and final hemming process. And the external force is greater in the final hemming than that in the pre hemming. This is because the larger the bending angle of the thin panel and the smaller the radius, the greater the reverse bending moment produced.
- (3) The concave edge structure retracts inward after pre hemming, and expand outward after final hemming. Compared with the case without adhesive, the surface wave of flange part of the hemming with adhesive is slightly larger, and the equivalent plastic strain in the bending and flanging regions decreases, which is related to the viscosity-pressure effect.
- (4) The normal force and the tangential force increase about 90 N and 30 N respectively, when the height increases by 1 mm. With the increase of the thickness of the adhesive layer, the external force decreases, especially when the normal force exceeds 0.3 mm. The external force with small radius ($R=140$ mm) concave and convex edge is

respectively increased by about 70 N and 100 N, compared with the straight edge.

Based on this model, more research work will be carried out in the future to study the influence of other parameters on the external hemming force, and finally to improve the manufacturing accuracy of autobody closure panels.

Acknowledgements

The authors sincerely thanks to the team members in our research group for their critical discussion and reading during manuscript preparation. The authors sincerely thanks to Professor Junying Min of Tongji University for providing the experimental platform.

Authors' contributions

JL completed the simulation and experiment analysis, and wrote the manuscript. WZ was in charge of framework and research methods of the whole manuscript. SW assisted with sampling and experiments. All authors read and approved the final manuscript.

Authors' Information

Jianjun Li, born in 1984, is currently a PhD candidate at *School of Mechanical Engineering, Tongji University, China*. He received his master degree from *Shandong University, China*, in 2011. His research interests include lightweight manufacturing of car body, material forming technology, mechanical behavior of materials and structures. E-mail: lijianjun@tongji.edu.cn

Wenfeng Zhu, born in 1976, is currently a professor at *School of Mechanical Engineering, Tongji University, China*. He received his PhD degree from *Shanghai Jiaotong University, China*, in 2005. His main research interests include advanced welding and connection technology, and mechanical behavior of materials and structures. E-mail: zhuwenfeng@tongji.edu.cn

Shunchao Wang, born in 1996, is currently a master candidate at *School of Mechanical Engineering, Tongji University, China*. E-mail: 2032760@tongji.edu.cn

Funding

Supported by National Natural Science Foundation of China (Grant Nos. 51975416 and 51275359).

Competing interests

The authors declare no competing financial interests.

Received: 13 August 2021 Revised: 15 December 2021 Accepted: 24 January 2022

Published online: 02 March 2022

References

- [1] A Andersson. Evaluation and visualisation of surface defects on auto-body panels. *Journal of Materials Processing Technology*, 2009, 209: 821–37.
- [2] P Martensson, D Zenkert, M Akermo. Method for cost and weight-efficient material diversity and partitioning of a carbon fibre composite body structure. *Proceedings of the Institution of Mechanical Engineers Part D-Journal of Automobile Engineering*, 2015, 230(1): 49–60.
- [3] S Gürgen. A parametric investigation of roller hemming operation on a curved edge part. *Archives of Civil and Mechanical Engineering*, 2019: 19(1): 11–19.
- [4] G Lin, J Li, S Hu, et al. A computational response surface study of three-dimensional aluminum hemming using solid-to-shell mapping. *Journal of Engineering Materials and Technology-Transactions of the ASME*, 2007: 129(2): 360–368.
- [5] H Livatyalı, T Laxhuber, T Altan. Improvement of hem quality by optimizing flanging and pre-hemming operations using computer aided die design. *Journal of Materials Processing Technology*, 2000, 98: 41–52.

- [6] G Zhang, X Wu, S J Hu. A study on fundamental mechanisms of warp and recoil in hemming. *Journal of Engineering Materials and Technology-Transactions of the ASME*, 2003, 123(4): 436–441.
- [7] G Wang, Z Gu, H Xu, et al. Numerical analysis and experimental investigation of surface defects in die hemming process. *International Journal of Material Forming*, 2019, 13: 91–102.
- [8] A Muderrisoglu, M Murata, M A Ahmetoglu, et al. Bending, flanging and hemming of sheet-experimental study. *Journal of Materials Processing Technology*, 1996, 59(1-2): 10–17.
- [9] N L Maoût, P Y Manach, S Thuillier. Influence of prestrain on the numerical simulation of the roller hemming process. *Journal of Materials Processing Technology*, 2012, 212(2): 450–457.
- [10] N L Maoût, S Thuillier, P Y Manach. Classical and roll-hemming processes of pre-strained metallic sheets. *Experimental Mechanics*, 2010, 50(7): 1087–1097.
- [11] X Hu, Z Q Lin, S Li, et al. Fracture limit prediction for roller hemming of aluminum alloy sheet. *Materials & Design*, 2011, 31(3): 1410–1416.
- [12] S Li, X Hu, Y Zhao, et al. Cyclic hardening behavior of roller hemming in the case of aluminum alloy sheets. *Materials & Design*, 2011, 32(4): 2308–2316.
- [13] S Thuillier, N L Maoût, P Y Manach. Numerical simulation of the roller hemming process. *Journal of Materials Processing Technology*, 2008, 198(1-3): 226–233.
- [14] E Eduardo, C Giuseppe, C Marco, et al. A dynamic compensation for roll hemming process. *IEEE Access*, 2018, 6: 18264–18275.
- [15] W G Drossel, M Pfeifer, M Findeisen, et al. The influence of the robot's stiffness on roller hemming processes. *ISR/Robotik, 41st International Symposium on Robotics*, Munich, Germany, June, 2014: 531–538.
- [16] H S Cho, J U Cho. The characteristics of shear adhesive interface fracture of aluminum foam DCB bonded using a single-lap method. *International Journal of Precision Engineering and Manufacturing*, 2014, 15(7): 1345–1350.
- [17] M F S F Moura, J P M Gonçalves, J A G Chousal, et al. Cohesive and continuum mixed-mode damage models applied to the simulation of the mechanical behaviour of bonded joints. *International Journal of Adhesion and Adhesives*, 2008, 28(8): 419–426.
- [18] M Svensson, K Mattiasson. Three-dimensional simulation of hemming with the explicit FE-Method. *Journal of Materials Processing Technology*, 2002, 128(1–3): 142–154.
- [19] J Li, W Zhu. Numerical simulation of the roller hemming process based on pressure-viscosity effect. *International Journal of Advanced Manufacturing Technology*, 2019, 105: 1023–1039.
- [20] P Burka, X Liu, M C Thompson. Modelling of adhesive bonding for aircraft structures applying the insertion squeeze flow method. *Composites Part B-Engineering*, 2013, 50(7): 247–252.
- [21] E Kara, A Kurşun, M R Haboğlu, et al. Fatigue behavior of adhesively bonded glass fiber reinforced plastic composites with different overlap lengths. *Proceedings of the Institution of Mechanical Engineers Part C-Journal of Mechanical Engineering Science*, 2015, 229(7): 1292–1299.
- [22] Y Lin, L Yang, S Liu, et al. Virtual simulation technology based research on subsoiling process. *Proceedings of the Institution of Mechanical Engineers Part C-Journal of Mechanical Engineering Science*, 2018, 233(5): 1989–1996.
- [23] K Gong, S Shao, H Liu, et al. Two-phase SPH simulation of fluid-structure interactions. *Journal of Fluids and Structures*, 2016, 65(8): 155–179.
- [24] M Hallajisany, J Zamani, J A Vitoria. Numerical and theoretical determination of various materials Hugoniot relations based on the equation of state in high-temperature shock loading. *High Pressure Research*, 2019, 39(4): 666–690.
- [25] V Abbas, K Morteza. Comparison of the numerical and experimental results of the sheet metal flange forming based on shell-elements types. *International Journal of Precision Engineering and Manufacturing*, 2011, 12(5): 857–863.
- [26] Y Y Cho, T W Kim. Development of algorithm for 3D mixed Elasto-Hydrodynamic lubrication analysis. *International Journal of Precision Engineering and Manufacturing*, 2011, 12(6): 1065–1070.

Submit your manuscript to a SpringerOpen[®] journal and benefit from:

- Convenient online submission
- Rigorous peer review
- Open access: articles freely available online
- High visibility within the field
- Retaining the copyright to your article

Submit your next manuscript at ► [springeropen.com](https://www.springeropen.com)